

# High brightness photonic band crystal semiconductor lasers in the passive mode locking regime

Cite as: Appl. Phys. Lett. **105**, 161101 (2014); <https://doi.org/10.1063/1.4899129>

Submitted: 01 July 2014 • Accepted: 11 October 2014 • Published Online: 20 October 2014

R. Rosales, V. P. Kalosha, K. Posilović, et al.



View Online



Export Citation



CrossMark

## ARTICLES YOU MAY BE INTERESTED IN

[1.9 W continuous-wave single transverse mode emission from 1060 nm edge-emitting lasers with vertically extended lasing area](#)

Applied Physics Letters **105**, 151105 (2014); <https://doi.org/10.1063/1.4898010>

[High-power single mode \( \$> 1W\$ \) continuous wave operation of longitudinal photonic band crystal lasers with a narrow vertical beam divergence](#)

Applied Physics Letters **92**, 103515 (2008); <https://doi.org/10.1063/1.2898517>

[Beam quality improvement of high-power semiconductor lasers using laterally inhomogeneous waveguides](#)

Applied Physics Letters **113**, 221107 (2018); <https://doi.org/10.1063/1.5054645>

 QBLOX



1 qubit

Shorten Setup Time

**Auto-Calibration**  
**More Qubits**

Fully-integrated

**Quantum Control Stacks**  
**Ultrastable DC to 18.5 GHz**  
Synchronized  $\ll 1$  ns  
Ultralow noise



100s qubits

[visit our website >](#)

# High brightness photonic band crystal semiconductor lasers in the passive mode locking regime

R. Rosales,<sup>1</sup> V. P. Kalosha,<sup>1</sup> K. Posilović,<sup>1,2</sup> M. J. Miah,<sup>1</sup> D. Bimberg,<sup>1</sup> J. Pohl,<sup>3</sup> and M. Weyers<sup>3</sup>

<sup>1</sup>*Institut für Festkörperphysik, Technische Universität Berlin, Hardenbergstrasse 36, 10623 Berlin, Germany*

<sup>2</sup>*PBC Lasers GmbH, Hardenbergstrasse 36, 10623 Berlin, Germany*

<sup>3</sup>*Ferdinand-Braun-Institut, Leibniz-Institut für Höchstfrequenztechnik, Gustav-Kirchhoff-Str. 4, Berlin 12489, Germany*

(Received 1 July 2014; accepted 11 October 2014; published online 20 October 2014)

High brightness photonic band crystal lasers in the passive mode locking regime are presented. Optical pulses with peak power of 3 W and peak brightness of about  $180 \text{ MW cm}^{-2} \text{ sr}^{-1}$  are obtained on a 5 GHz device exhibiting 15 ps pulses and a very low beam divergence in both the vertical and horizontal directions. © 2014 AIP Publishing LLC.

[<http://dx.doi.org/10.1063/1.4899129>]

High brightness picosecond pulsed lasers in the 1064 nm range are currently attracting much attention, most of which is directed towards emerging applications in materials processing as well as in advanced imaging techniques for biology and medicine.<sup>1–3</sup> Owing to their excellent beam quality, high brightness picosecond pulses can be more tightly focused at the target plane, while also providing a greater depth of field with less stringent focusing optics requirements. Semiconductor laser based systems are advantageous as compared to commercially available Ti:sapphire and fiber lasers owing to their higher efficiency, compactness, wavelength tunability, as well as the reduced complexity and footprint of laser diodes, although at the expense of a reduced brightness, which still needs to be increased. Some approaches are known to improve the brightness of a laser diode.<sup>4–7</sup> Most of them are based on an expansion of the waveguide dimensions to increase the output power and methods for ensuring single mode emission to obtain a high beam quality. Regarding the waveguide expansion along the vertical direction (direction of the epitaxial growth), AlGaAs/GaAs/InGaAs quantum-well heterostructures with a thick layer below the active region, having a refractive index close to the effective index of the fundamental mode, achieve output powers of up to 0.5 W in continuous wave (CW) in a transverse single mode ridge waveguide.<sup>8</sup> Ultra-wide waveguides based on AlGaAs/GaAs/InGaAs quantum-well heterostructures with a multitude of vertically guided modes could also generate a single fundamental vertical mode by asymmetric positioning of the active layers with respect to the waveguide center.<sup>9</sup> This asymmetric positioning results in a substantial decrease of the confinement factors for the higher order modes and provides guiding selection of the fundamental one. By using this approach, pulses of 12.4 ps at a repetition rate of 13 GHz with a peak power of 0.9 W and peak brightness of  $50 \text{ MW cm}^{-2} \text{ sr}^{-1}$  under passive mode locking have been reported,<sup>10</sup> also showing far field full width at half maximum (FWHM) angles of about  $15^\circ$  and  $9^\circ$  in the vertical and lateral directions, respectively. These methods for achieving high brightness emission, however, suffer from growth precision issues of the expanding and active layers which in turn lead to a less

effective mode selection. The same refers to temperature effects, which change the refractive index ratio of the epitaxial layers therefore modifying the modal content of the output beam. Regarding methods for improving the brightness in the lateral direction, the best approach to date is that of the tapered laser. With such a design, optical pulses with more than 6.3 W peak power having 74 ps duration have been obtained by modulating the device with a GHz sinusoidal current.<sup>11</sup> The major disadvantage of this structure is the underlying scheme for mode filtering which is achieved solely by a conventional narrow stripe. Hence, by increasing the output power, nonlinear effects such as filamentation and self-focusing take place, reducing the laser beam quality.<sup>12</sup>

In this letter, we overcome the previous limitations by using ultra-broad waveguide lasers consisting of multiple vertically stacked layers of alternating refractive indices, which we refer to as longitudinal photonic band crystal (PBC) lasers,<sup>13–20</sup> and investigate the laser performance in the passive mode locking regime. The multilayer structure provides an expansion of the fundamental mode over the whole waveguide in order to obtain a very low beam divergence. The epitaxial structure was grown by metal-organic vapour phase epitaxy (MOCVD) on a GaAs substrate. The laser waveguide thickness is about  $11 \mu\text{m}$  which includes ten layers of alternating  $\text{Al}_{0.2}\text{Ga}_{0.8}\text{As}/\text{Al}_{0.35}\text{Ga}_{0.65}\text{As}$  with graded index interfaces and a stack of four InGaAs/GaAsP quantum wells as the active region. The structure was doped using C on the p-side and Si on the n-side. Fig. 1(a) shows the transverse refractive index profile along the laser vertical direction together with the electric field magnitude of the fundamental (solid line) and first higher order (dashed line) modes. The modes are obtained from simulations based on the scalar wave equations along the multi-layered waveguide with the given transverse refractive index profile.<sup>18</sup> A specially designed sequence of alternating layers having thicknesses of 1020 nm and 70 nm, respectively, and a 20-nm thick graded-index layer at their interfaces provide the expansion of the fundamental mode with the largest confinement factor in the active region as compared to that of multiple higher order modes. In addition, it discriminates the higher order modes by their substantially higher optical

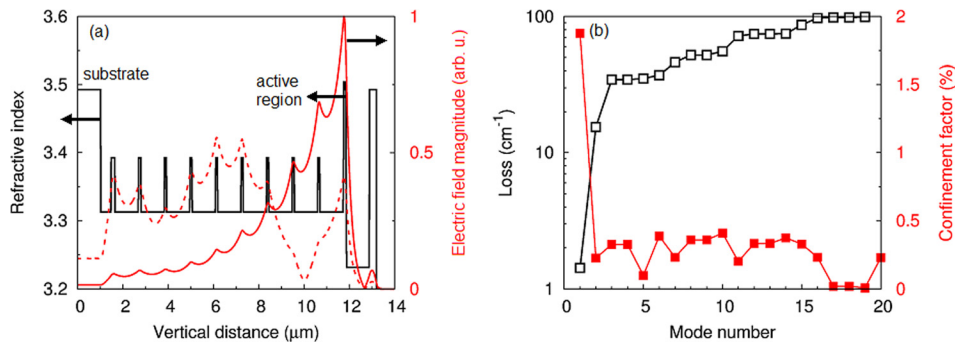


FIG. 1. (a) Refractive index profile and simulated electric field magnitudes for the fundamental (solid line) and first higher order (dashed) modes based on the scalar wave equations. (b) Calculated optical losses (empty squares) and confinement factor (solid squares) of the first 20 modes.

losses. The discrimination by losses is enhanced by a modification of the periodicity within the layer pairs closest to the substrate, which results in large leakage of all higher order modes.<sup>18</sup> Furthermore, non-uniform doping profiles with larger doping concentration were used in the areas of predominant localization of the higher order modes in order to increase their losses via free-carrier absorption. As a result, the fundamental mode of the laser waveguide under consideration has a confinement factor of about an order of magnitude larger (Fig. 1(b), solid squares) and losses of about an order of magnitude smaller (Fig. 1(b), empty squares) than the rest of the higher order modes, as calculated from the same simulation results of the scalar wave equation. Because of the mode selection in favour of the fundamental mode, which is expanded into the vertically broad-area waveguide, the output radiation is single-mode and exhibits a single-lobe far field with a very low beam divergence in the vertical direction. Since the power density per facet area is decreased upon broadening the waveguide and immunity to most of the limiting nonlinear optical effects is increased, the maximum output peak power and hence the laser peak brightness are increased.

The internal characteristics of the laser structure were assessed using 100 μm stripe broad area lasers of different cavity lengths under pulsed operation at 20 °C, using electric pump pulses with a duration of 800 ns at a repetition rate of 1 kHz. The inverse of the differential quantum efficiency  $\eta_{\text{diff}}$  is plotted in Fig. 2(a) as a function of cavity length  $L$  from which the internal quantum efficiency of 93% and internal

losses of 1.4 cm<sup>-1</sup> were estimated. The threshold modal gain  $\Gamma g_0$  and threshold current density at  $L = \infty$  ( $j_{\text{inf}}$ ) are deduced from Fig. 2(b) at 34 cm<sup>-1</sup> and 230 A cm<sup>-2</sup>, respectively. Ridge waveguide lasers having a width of 5 μm have been used for assessing the far field profiles in both the vertical and horizontal directions. Figure 3 shows typical profiles under continuous wave excitation at 500 mA, demonstrating single-mode operation and a small vertical far field divergence with a full width at half maximum (FWHM) of only 9° with an almost circular beam profile. Ridge waveguide lasers consisting of two electrically isolated sections (gain and saturable absorber) having different cavity lengths have been processed for passively mode locked operation. The ratio of the gain to absorber section lengths has been optimized for optical pulse emission, being in most cases ~12:1. All lasers are as-cleaved and have been mounted p-side up on copper blocks. Mode locking in these devices was first investigated by measurements of the laser autocorrelation intensity obtained by the nonlinear process of second harmonic generation (SHG).<sup>21</sup> The minimum pulse duration (after deconvolution assuming a Gaussian pulse shape), for three different cavity lengths is shown in Fig. 4. As can be observed, the pulse width increases with increasing cavity length, a trend that can be attributed to a larger amount of intracavity dispersion in longer devices as well as to a decrease in pulse stability owing to an increase in the number of round trips to achieve mode locking. The maximum average power in all devices was ~300 mW before thermal rollover or catastrophic optical mirror damage occurred. This leaves room

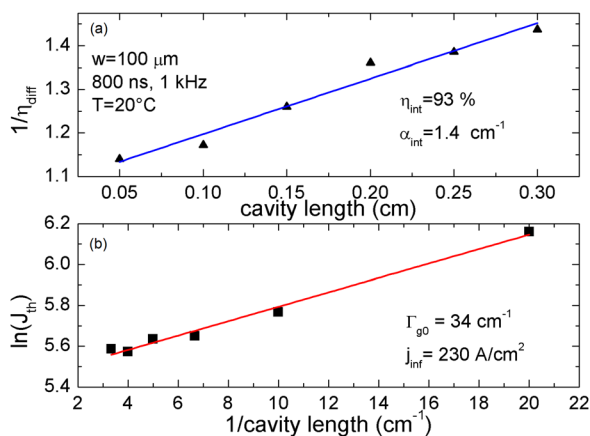


FIG. 2. (a) Inverse differential efficiency vs. cavity length and (b) threshold current density vs. inverse length of 100 μm broad area lasers in pulsed operation at 20 °C (electric pump pulse duration = 800 ns, repetition rate = 1 kHz).

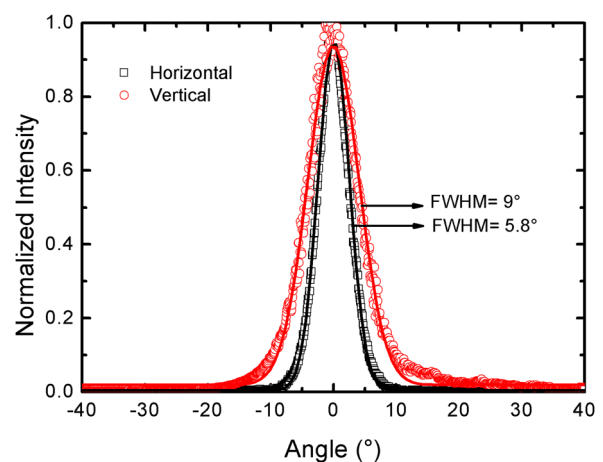


FIG. 3. Typical far field profiles and Gaussian fits (solid line) from ridge waveguide lasers (5 μm stripe and 1 mm length) under continuous wave operation at 500 mA.

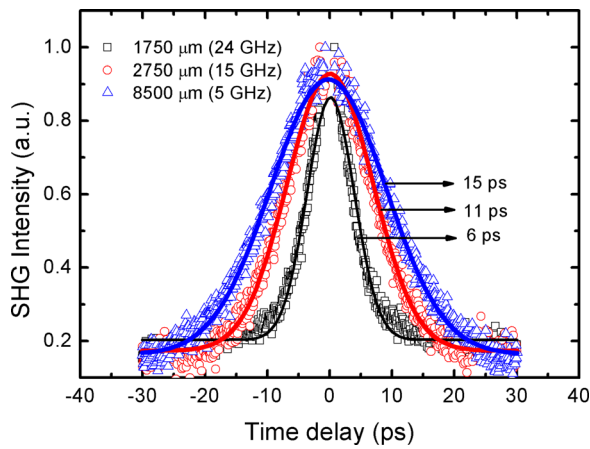


FIG. 4. SHG intensity and Gaussian fits (solid lines) from three different cavity lengths corresponding to the minimum pulse duration for each case.

for improvement by proper p-down mounting for efficient heat extraction as well as by suitable facet coatings. Specifically, for the 8500  $\mu\text{m}$  long (4.8 GHz) device, the minimum pulse width was obtained at a current of  $I_{\text{gain}} = 1140 \text{ mA}$  in the gain section and a reverse bias of  $V_{\text{abs}} = -0.6 \text{ V}$  in the absorber section, for an average power of 215 mW. At this bias condition, a pulse peak power of 3 W was obtained. The laser emission is nearly diffraction limited, with a  $M^2$  factor ranging between 1.15 and 1.2 in the lateral direction and between 1.2 and 1.25 in the vertical direction for all applied bias conditions. At the maximum peak output power of 3 W, this results in a pulse brightness of  $\sim 180 \text{ MW cm}^{-2} \text{ sr}^{-1}$ , representing the highest value ever achieved for a passively mode locked, electrically pumped laser diode at 1060 nm. The laser radio frequency (RF) spectrum in Fig. 5 further confirms the mode locked operation by the sharp peaks at the corresponding repetition frequency and subsequent harmonics, indicative of a pure mode-locking regime without Q-switching instabilities. The fundamental RF line has a linewidth of  $\sim 400 \text{ kHz}$ , demonstrating pulse stability and relatively low jitter of the optical pulses. The optical spectrum at the same bias condition exhibits an almost Gaussian shape with a FWHM of 1.2 nm (Fig. 6), which results in a time bandwidth product of 5, revealing strongly chirped pulses due to the inherent coupling of the

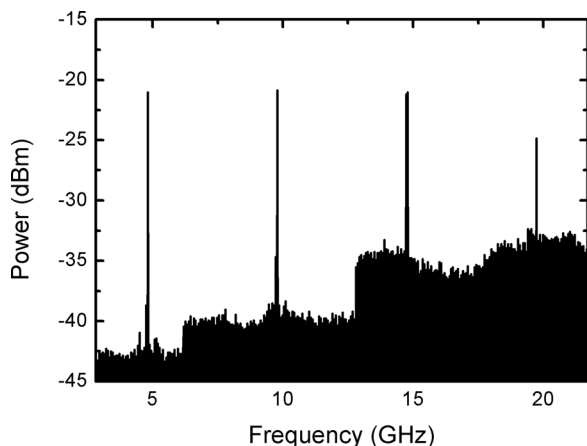


FIG. 5. Full span RF spectrum of the 5 GHz laser under mode locked regime at  $I_{\text{gain}} = 1140 \text{ mA}$ ,  $V_{\text{abs}} = -0.6 \text{ V}$ .

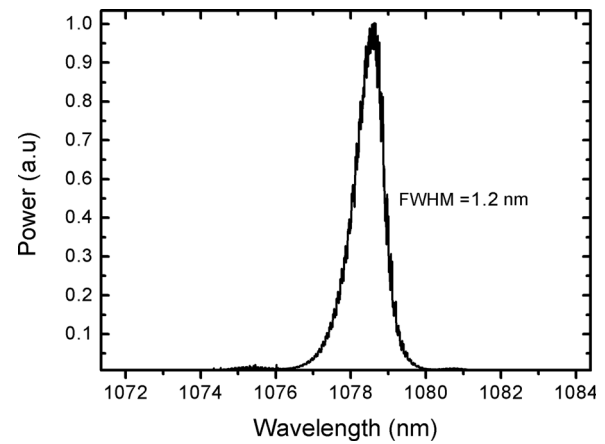


FIG. 6. Optical spectrum of the 5 GHz laser under mode locked regime at  $I_{\text{gain}} = 1140 \text{ mA}$ ,  $V_{\text{abs}} = -0.6 \text{ V}$ .

optical gain and the refractive index in semiconductor lasers. This chirp could be compensated externally through a dispersive medium, prism pair, or grating pair, provided it is linear, as already reported for different types of semiconductor mode locked lasers.<sup>22–24</sup> In such a case, pulses as narrow as 1.5 ps, with a peak power of 30 W and a peak brightness of  $1.8 \text{ GW cm}^{-2} \text{ sr}^{-1}$  would be attained. Further work will be devoted to investigating these effects.

In conclusion, we have demonstrated the potential of a laser diode design for the generation of short optical pulses with high peak brightness in the 1060 nm range. The devices can be used directly in applications requiring GHz picosecond pulses with Watt peak power levels. The low beam divergence, almost circular beam profile and their high brightness, also make them ideal seed sources for efficient master-oscillator-fiber-amplifier schemes requiring high coupling efficiency and a reduced number of amplifiers for stable and low cost high power pulsed systems.

The research leading to these results has received funding from the DFG in the framework of the SFB 787.

- <sup>1</sup>J. Cheng, W. Perrie, M. Sharp, S. P. Edwardson, N. G. Semaltianos, G. Dearden, and K. G. Watkins, *Appl. Phys. A* **95**, 739 (2009).
- <sup>2</sup>H. Yokoyama, A. Sato, H.-C. Guo, K. Sato, M. Mure, and H. Tsubokawa, *Opt. Express* **16**, 17752 (2008).
- <sup>3</sup>Y. Kusama, Y. Tanushi, M. Yokoyama, R. Kawakami, T. Hibi, Y. Kozawa, T. Nemoto, S. Sato, and H. Yokoyama, *Opt. Express* **22**, 5746 (2014).
- <sup>4</sup>J. J. Lim, S. Sujecki, L. Lang, Z. Zhang, D. Paboeuf, G. Pauliat, G. Lucas-Leclin, P. Georges, R. MacKenzie, P. Bream, S. Bull, K.-H. Hasler, B. Sumpf, H. Wenzel, G. Erbert, B. Thestrup, P. M. Petersen, N. Michel, M. Krakowski, and E. C. Larkins, *IEEE J. Sel. Top. Quantum Electron.* **15**, 993 (2009).
- <sup>5</sup>B. Thestrup, M. Chi, B. Sass, and P. M. Petersen, *Appl. Phys. Lett.* **82**, 680 (2003).
- <sup>6</sup>L. Liu, H. Qu, Y. Wang, Y. Liu, Y. Zhang, and W. Zheng, *Opt. Lett.* **39**, 3231 (2014).
- <sup>7</sup>R. Parke, D. F. Welch, A. Hardy, R. Lang, D. Mehuys, S. O'Brien, K. Dzurko, and D. Scifres, *IEEE Photonics Technol. Lett.* **5**, 297 (1993).
- <sup>8</sup>A. P. Bogatov, T. I. Gushchik, A. E. Drakin, A. P. Nekrasov, and V. V. Popovichev, *Quantum Electron.* **38**, 935 (2008).
- <sup>9</sup>N. A. Pikhtin, S. O. Slipchenko, Z. N. Sokolova, A. L. Stankevich, D. A. Vinokurov, I. S. Tarasov, and Z. I. Alferov, *Electron. Lett.* **40**, 1413 (2004).
- <sup>10</sup>O. Brox, T. Prziwarka, A. Klehr, F. Bugge, M. Matalla, H. Wenzel, and G. Erbert, *Semicond. Sci. Technol.* **28**, 045015 (2013).

- <sup>11</sup>A. Klehr, B. Sumpf, K.-H. Hasler, J. Fricke, A. Liero, and G. Erbert, *IEEE Photonics Technol. Lett.* **22**, 832 (2010).
- <sup>12</sup>H. Odriozola, J. M. G. Tijero, L. Borrueal, I. Esquivias, H. Wenzel, F. Dittmar, K. Paschke, B. Sumpf, and G. Erbert, *IEEE J. Quantum Electron.* **45**, 42 (2009).
- <sup>13</sup>N. N. Ledentsov and V. A. Shchukin, *Opt. Eng.* **41**, 3193 (2002).
- <sup>14</sup>M. V. Maximov, Y. M. Shernyakov, I. I. Novikov, S. M. Kuznetsov, L. Y. Karachinsky, N. Y. Gordeev, V. P. Kalosha, V. A. Shchukin, and N. N. Ledentsov, *IEEE J. Quantum Electron.* **41**, 1341 (2005).
- <sup>15</sup>I. I. Novikov, L. Y. Karachinsky, M. V. Maximov, Y. M. Shernyakov, S. M. Kuznetsov, N. Y. Gordeev, V. A. Shchukin, P. S. Kop'ev, N. N. Ledentsov, U. Ben-Ami, V. P. Kalosha, A. Sharon, T. Kettler, K. Posilovic, D. Bimberg, V. Mikhelashvili, and G. Eisenstein, *Appl. Phys. Lett.* **88**, 231108 (2006).
- <sup>16</sup>D. Bimberg, K. Posilovic, V. Kalosha, T. Kettler, D. Seidlitz, V. A. Shchukin, N. N. Ledentsov, N. Y. Gordeev, L. Y. Karachinsky, I. I. Novikov, M. V. Maximov, Y. M. Shernyakov, A. V. Chunareva, F. Bugge, and M. Weyers, *Proc. SPIE* **7616**, 76161I (2010).
- <sup>17</sup>T. Kettler, K. Posilovic, L. Y. Karachinsky, P. Ressel, A. Ginolas, J. Fricke, U. W. Pohl, V. A. Shchukin, N. N. Ledentsov, D. Bimberg, J. Jonsson, M. Weyers, G. Erbert, and G. Trankle, *IEEE J. Sel. Top. Quantum Electron.* **15**, 901 (2009).
- <sup>18</sup>V. P. Kalosha, K. Posilovic, T. Kettler, V. A. Shchukin, N. N. Ledentsov, and D. Bimberg, *Semicond. Sci. Technol.* **26**, 075014 (2011).
- <sup>19</sup>V. Kalosha and D. Bimberg, U.S. patent application 14169520 (February 2014).
- <sup>20</sup>R. Rosales, D. Arsenijevic, K. Posilovic, V. P. Kalosha, M. J. Miah, D. Bimberg, J. Pohl, and M. Weyers, in *High Power Diode Lasers and Systems Conference (HPD)* (IEEE, 2013), pp. 24–25.
- <sup>21</sup>H. P. Weber, *J. Appl. Phys.* **38**, 2231 (1967).
- <sup>22</sup>M. Schell, M. Tsuchiya, and T. Kamiya, *IEEE J. Quantum Electron.* **32**, 1180 (1996).
- <sup>23</sup>H. Schmeckeber, G. Fiol, C. Meuer, D. Arsenijevic, and D. Bimberg, *Opt. Express* **18**, 3415 (2010).
- <sup>24</sup>R. Rosales, S. G. Murdoch, R. T. Watts, K. Merghem, A. Martinez, F. Lelarge, A. Accard, L. P. Barry, and A. Ramdane, *Opt. Express* **20**, 8649 (2012).